IV Escola de Primavera de Transição e Turbulência
Universidade Federal do Rio Grande do Sul
Pontifícia Universidade Católica do Rio Grande do Sul
Porto Alegre, RS, 27 de setembro a 1º de outubro de 2004

LARGE EDDY SIMULATION OF THREE-DIMENSIONAL TURBULENT FLOWS BY THE FINITE ELEMENT METHOD

Adriane Prisco Petry
Department of Mechanical Engineering
Federal University of Rio Grande do Sul
Sarmento Leite, 425, CEP:90050-170, Porto Alegre, RS, Brazil
adrianep@mecanica.ufrgs.br

Armando Miguel Awruch
Graduate Program in Civil Engineering
Federal University of Rio Grande do Sul
Osvaldo Aranha, 99, CEP:90035-190, Porto Alegre, RS, Brazil
awruch@adufrgs.ufrgs.br

Abstract: Formulation, implementation and applications of a numerical algorithm to simulate turbulent, incompressible, isothermal flows are the main objectives of this work. The transient three-dimensional flow is analyzed using an explicit Taylor-Galerkin scheme and the finite element method with hexahedrical eight-node element. Turbulence is simulated using Large Eddy Simulation. For sub-grid scales two models were implemented, the classical Smagorinsky´s model and the dynamic eddy viscosity model. For the second filtration, which is necessary in the dynamic model, a new method was developed based on independent finite elements that involve each node in the original mesh. The implemented scheme is efficient and good results with low additional computational cost were obtained. Results for two classical problems, the driven cavity and the backward facing step are presented. Comments about the model applicability for flows with high Reynolds numbers are also presented.

Keywords: Turbulence, Large Eddy Simulation, Dynamic Model, Finite Element Method, Computational Fluid Dynamics

1. Introduction

Flow analysis is an important subject for several engineering fields, as well as in other areas of science and technology. Many problems are characterized by turbulent flows and suitable models are necessary to represent flow characteristics.

Turbulent flows are usually characterized by high Reynolds numbers, a coherent behavior at large scales level and random behavior at small scales. They are also diffusive, three-dimensional and transient (Tenekes and Lumley, 1972). Another important characteristic of turbulent flows is that multiple scales are involved (Silveira Neto, 2002), however even small scales are usually greater than the scales of molecular movement (Hinze, 1975), consequently turbulence may be described as a continuous phenomenon.

Using the conservation equations of mass, energy and momentum, a complex system of partial differential equations is obtained. Computational Fluid Dynamics, is an important methodology to solve the problem. Different numerical methods are used to carried out these simulations. The Finite Element Method (Hughes, 1987; Reddy and Gartling, 1994) is an efficient technique for the analysis of problems with complex geometry. This methodology was adopted in the present work.

The conservation equations of fluid mechanics represents a mathematical model, which is able to describe turbulent fluid flows. However, the required discretization in space and time to simulate all scales directly (Direct Simulation), becomes impracticable this type of analysis, for most of practical problems. This is a consequence of the large number of equations to be solved (Grötsbach, 1987), leading to very large processing times, even for the most advanced computers (Kim and Menon, 1999). As a consequence of the impossibility to apply Direct Simulation for a large range of problems, it is necessary to use alternative methodologies, such as the classic models based on the solution of the Reynolds Average Equations (Hinze, 1975) and the Large Eddy Simulation (Ferziger 1993, Rogallo and Moin 1984, Lesieur et al, 1995).

In the Large Eddy Simulation technique, the conservation equations are solved for large flow scales directly and models are used to represent the effects of the subgrid scales. These models have the same purpose of the conventional turbulence models, but they may be very simple because they consider only the effect of small scales. Moreover, subgrid models have minor geometry dependence, therefore the small scales are of more universal nature than the total turbulence.

This work presents the formulation, implementation and application of a numerical algorithm for three-dimensional, turbulent flow analysis. More details may be found in Petry, 2002. The methodology is based on the Finite Element Method and Large Eddy Simulation. A computational code to simulate transient, quasi-incompressible, three-dimensional flows, was developed using an explicit Taylor-Galerkin scheme, with eight-node hexahedrical element.

Two different subgrid models were implemented: the Smagorinsky´s model (Smagorinsky, 1963) and the dynamic model (Germano et al., 1991; Lilly, 1992). The dynamic model implementation implies in a second filter operation. It was developed a new methodology for this process, called *Second Filter by Independent Finite Elements*. Simulations of the backward-facing step and the driven cavity flows are presented in this work. These simulations confirm the validity of the implemented scheme, however they also demonstrate that improvements are necessary to overcome difficulties presented to simulate large computational problems.

2. Mathematical and Numerical Aspects

2.1 Governing Equations

Incompressible flows are analyzed, consequently it is necessary to adopt some scheme to overcome difficulties in the numerical analysis of these kind of flows (Awruch and Petry, 1997, Reddy and Gartling, 1994). Usual formulation for incompressible flow is based on the assumption of a constant value for the density and, from this hypothesis, it is deduced that the speed of sound in the flow field is infinite (Schlichting, 1968), however in real flows the propagation of sound always occurs with a finite speed. In the present work, the equations for a quasi-incompressible flow are adopted (Kawahara and Hirano, 1983), which assume constant density, but a finite value for the speed of sound. With this consideration the equation of mass conservation contains the time derivative of pressure.

From the equations of conservation of mass, energy and momentum for three-dimensional, transient, isothermal, quasi-incompreessible viscous flows of a Newtonian fluid (White, 1974, Kawahara and Hirano, 1983), the equations for Large Eddy Simulation are deduced (Petry 2002).

In a Large Eddy Simulation (Findikakis and Street, 1982) each field variable is decomposed into large scale field (identified by the over-bar) and subgrid scale field (identified by the apostrophe):

$$v_i = \overline{v_i} + v_i' \qquad p = \overline{p} + p' \qquad \rho = \overline{\rho} + \rho' \tag{1}$$

Since density is constant, then $\rho' = 0$.

After the filtering process of the equations of conservation of mass and momentum of the isothermal, viscous, quasi-incompressible, three-dimensional and transient flow, the governing equations are given by:

$$\frac{\partial \overline{p}}{\partial t} + C^2 \frac{\partial}{\partial x_j}\left(\rho \overline{v}_j\right) = 0 \tag{2}$$

$$\begin{aligned} &\frac{\partial}{\partial t}\left(\rho \overline{v}_i\right) + \frac{\partial}{\partial x_j}\left(\rho \overline{v}_i \overline{v}_j\right) + \frac{\partial \overline{p}}{\partial x_j}\delta_{ij} - \frac{\partial}{\partial x_j}\left\{\nu\left(\frac{\partial}{\partial x_j}(\rho \overline{v}_i) + \frac{\partial}{\partial x_i}(\rho \overline{v}_j)\right) + \frac{\lambda}{\rho}\left(\frac{\partial}{\partial x_k}(\rho \overline{v}_k)\right)\delta_{ij}\right\} \\ &\quad + \frac{\partial}{\partial x_j}\left\{\rho\left(L_{ij} + C_{ij} + \overline{v_i' v_j'}\right)\right\} - f_i = 0 \qquad (i, j, k = 1,2,3) \text{ in } \Omega \end{aligned} \tag{3}$$

With the following boundary conditions:

$$v_i = \hat{v}_i \qquad (i = 1,2,3) \text{ in } \Gamma_v \tag{4}$$

$$\left\{\left[-\overline{p} + \frac{\lambda}{\rho}\frac{\partial}{\partial x_k}\left(\rho \overline{v_k}\right)\right]\delta_{ij} + \nu\left[\frac{\partial}{\partial x_j}\left(\rho \overline{v_i}\right) + \frac{\partial}{\partial x_i}\left(\rho \overline{v_j}\right)\right]\right\} n_j = t_i \qquad (i, j, k = 1,2,3) \text{ in } \Gamma t \tag{5}$$

and the corresponding initial conditions:

$$v_i = \hat{v}_{i0} \qquad (i, j, k = 1,2,3) \text{ in } \Omega \tag{6}$$

$$p = \hat{p}_0 \qquad \text{in } \Omega \tag{7}$$

Where:
ρ - density
x_i –coordinate, i=1,2,3
δ_{ij} - Kroenecker delta
n_j – cossin of the ngle formed by the normal vector to the boundary with the axis x_j
t_i – prescribed values of surface forces at the boundary
λ - volumetric viscosity

C- sound propagation speed

ν -cinematic viscosity.

$\overline{v}_i$ -large scale velocity component in the direction of the axis x_i

$\overline{p}$ - large scale pressure component

v'_i - subgrid scale velocity component in the direction of the axis x_i

$L_{ij} = \overline{\overline{v}_i \overline{v}_j} - \overline{v}_i \overline{v}_j$, Leonard´s terms

$Cij = \overline{\overline{v}_i v_j'} + \overline{v_i' \overline{v}_j}$, Crossed terms

$\overline{v_i' v_j'}$ subgrid Reynolds stress components

$\hat{v}_i$ - prescribed values of velocity at the boundary

The terms L_{ij} and C_{ij} can be neglected (Findikakis and Street, 1982). Previous studies (Petry and Awruch, 1997b) confirm that the consideration of these terms have not significant influence and increase around 20% the processing time.

Equations (2) and (3), neglecting the Leonard´s and crossed terms, with the boundary and initial conditions given by Equations (4), (5), (6) and (7), are the governing equations of the turbulent, isothermal, quasi-incompressible flow, of a Newtonian fluid. Adding the subgrid scale model equations, the system to be solved is obtained.

2.2 Subgrid Scale Models

The two implemented models are based on the eddy viscosity concept. Using the hypothesis of Bousinesq, the subgrid Reynolds stresses are given by:

$$-\overline{v_i' v_j'} = \nu_t \left(\frac{\partial \overline{v}_i}{\partial x_j} + \frac{\partial \overline{v}_j}{\partial x_i} \right) \tag{8}$$

where ν_t is the eddy viscosity.

This is the original equation of Bousssinesq. Usually for incompressíble flows the Equation (8) is modified (Hinze, 1975), introducing a term with the subgrid kinetic energy to make the model compatible with the usual equation of mass conservation for incompressible flows (div **v**=0). However in this work the continuity equation is the modified one, for quasi-incompressible flows (Equation (2)), therefore, Equation (8) is used without any additional term.

2.3 Smagorinsky´s Model

The model of Smagorinsky (1963) has been traditionally used to represent the effect of the subgrid scales in Large Eddy Simulation (Findikakis and Street, 1983; Lesieur et al, 1995). It is a eddy viscosity model in which the subgrid Reynolds stresses are given by the Equation (8) and eddy viscosity is defined as:

$$\nu_t = C_S{}^2 \overline{\Delta}^2 \left| \overline{S} \right| \tag{9}$$

where C_S is the Smagorinsky´s constant, with varying values from 0.1 to 0.22, and the other terms are given by:

$$\left| \overline{S} \right| = \sqrt{2 \overline{S}_{ij} \overline{S}_{ij}} \tag{10}$$

$$\overline{S}_{ij} = \frac{1}{2} \left(\frac{\partial \overline{v}_i}{\partial x_j} + \frac{\partial \overline{v}_j}{\partial x_i} \right) \tag{11}$$

$$\overline{\Delta} = \sqrt[3]{\prod_{i=1}^{3} \Delta x_i} \tag{12}$$

2.4 Eddy Viscosity Dynamic Model

The dynamic model was first proposed by Germano et al., 1991, and modified by Lilly, 1992. The subgrid Reynolds stresses are also obtained with Equation (8), but the eddy viscosity is defined by:

$$\nu_t = C(\mathbf{x}, t) \overline{\Delta}^2 \left| \overline{S} \right| \tag{13}$$

The dynamic coefficient, C(**x**, t), is calculated as a function of the local flow characteristics, using a double filtering process and it is based on information of the small scales solved by the mesh, defined as:

$$C(\mathbf{x},t) = -\frac{1}{2}\frac{L_{ij}M_{ij}}{M_{ij}M_{ij}} \tag{14}$$

where Lij e Mij are given by:

$$L_{ij} = \left\langle \overline{v}_i \overline{v}_j \right\rangle - \left\langle \overline{v}_i \right\rangle \left\langle \overline{v}_j \right\rangle \qquad M_{ij} = \left\langle \overline{\Delta} \right\rangle^2 \left| \left\langle \overline{S}_{ij} \right\rangle \right| \left\langle \overline{S}_{ij} \right\rangle - \left\langle \overline{\Delta}^2 \left| \overline{S}_{ij} \right| \overline{S}_{ij} \right\rangle \tag{15}$$

$$\left\langle \overline{S}_{ij} \right\rangle = \frac{1}{2}\left(\frac{\partial \left\langle \overline{v}_i \right\rangle}{\partial x_j} + \frac{\partial \left\langle \overline{v}_j \right\rangle}{\partial x_i} \right) \qquad \left| \left\langle \overline{S} \right\rangle \right| = \sqrt{2 \left\langle \overline{S}_{ij} \right\rangle \left\langle \overline{S}_{ij} \right\rangle} \tag{16}$$

$\left\langle \overline{\Delta} \right\rangle$ - characteristic length of the second filter, with $\left\langle \overline{\Delta} \right\rangle > \overline{\Delta}$.

In the above equations, the bar indicates the first filtering process (filter at mesh level) and the symbol $\langle\ \rangle$ indicates the second filtering process (test filter).

For the solution of the system of equations, the Finite Element Method is employed. To get the system of algebraic equations, time derivatives are expanded in Taylor series, including the second order terms, and for the space discretization the classic Galerkin method is applied (Reddy and Gartling, 1994). To save processing time, analytical expressions for the elements matrices are used and the hexaedrical isoparametric element (Burbridge e Awruch,2000). This scheme is known as Taylor-Galerkin, (Donea, 1984), and was used by Azevedo, 1999, for the simulation of three-dimensional laminar flows with fluid-structure interaction. The scheme is explicit and conditionally stable and the integration time step has the following restriction:

$$\Delta t \le \frac{\Delta x_i(\min)}{C + V} \tag{17}$$

where $\Delta x_i(\min)$ is the minimum dimension of the mesh elements, C is the speed of sound and V is the reference velocity. Details of the numerical methodology can be found in Petry, 2002, and Azevedo, 1999.

2.5 The Second Filter: Proposed Methodology

The Equation (14) defines the dynamic coefficient, C(**x**, t). This coefficient depends on the use of two filters of different characteristic lengths. The first filter, at the mesh level, has characteristic length related to element dimension. For the second filtering process (test filter) the characteristic length must be greater than the length of the first filter. Based on these two scale levels, the dynamic model uses information of the smallest resolved scales (situated between the two filters) to calculate the dynamic coefficient employing Equations (14), (15) and (16).

For the second filtering process many proposals have been presented. Oshima, et al., 1996, formulate the second filtering operation in a Finite Element code using expansions in Taylor series. Padilla and Silveira Neto, 2000, present and compare different methodologies in the context of Finite Volumes.

The new methodology used in this work was presented in Petry, 2002. The *Second Filter by Independent Finite Elements* uses techniques common to finite elements, such as: the definition of elements by conectivities; the use of two systems of coordinates (global (x_1,x_2,x_3) and natural (ξ,η,ζ)); the transformations of coordinates and elements interpolation functions. The scheme consists in the generation of one super-element around each node of the mesh, then, with the usual shape functions, a linear interpolation of the variables at the super-element nodes is performed to get filtered values in the corresponding internal node.

The first stage is included in the pre-processing phase, and consists of generating a list of conectivities of the independent super-elements for each node.. In this scheme the test filter dimension is not prescribed, but it is possible to include some restriction with respect to such dimension. In Figure 1 an example of an independent super-element, with its corresponding internal node, is presented.

The second stage, also included in the pre-processing phase to reduce additional computational cost., is to evaluate the natural coordinates (ξ_I, η_I, ζ_I) of node I in the interior of its independent super-element. Global coordinates of a point I inside of an element can be calculated by the following transformation of coordinates:

$$(x_i)_I = \sum_{\alpha=1}^{8} \Psi_\alpha(\xi_I, \eta_I, \zeta) x_{i\alpha} \tag{18}$$

This is the usual transformation used in finite elements, where

$(x_i)_I$ - coordinate of any point I inside an independent super-element, (i=1,2,3)

$x_{i\alpha}$ - coordinate of node α, (α =1,2,3,4,5,6,7,8), (i=1,2,3)

$\psi_\alpha(\xi_I, \eta_I, \zeta_I)$ - interpolation function of node α, evaluated at point I, with natural coordinates (ξ_I, η_I, ζ_I)

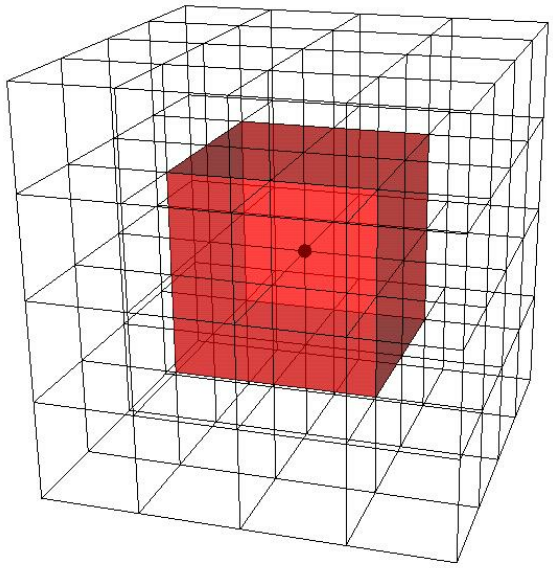

Figure 1 – Independent Super-Element created around a node, to be used in the second filtering process.

The interpolation functions for a isoparametric eight node hexahedrical element are given by

$$\{\Psi^e\} = \frac{1}{8}\begin{Bmatrix} (1-\xi)(1-\eta)(1-\zeta) \\ (1+\xi)(1-\eta)(1-\zeta) \\ (1+\xi)(1+\eta)(1-\zeta) \\ (1-\xi)(1+\eta)(1-\zeta) \\ (1-\xi)(1-\eta)(1+\zeta) \\ (1+\xi)(1-\eta)(1+\zeta) \\ (1+\xi)(1+\eta)(1+\zeta) \\ (1-\xi)(1+\eta)(1+\zeta) \end{Bmatrix} \tag{19}$$

It is necessary to solve the inverse problem represented by Equation (18), to obtain the natural coordinates of a point inside the element (ξ_I, η_I, ζ_I), from its global coordinates, $(x_1,x_2,x_3)_I$, and the global coordinates of the eight nodes of the super-element, $(x_1,x_2,x_3)_\alpha$.

In the analysis of this problem, a non linear system with three equations is derived and an algorithm using an iterative process of solution was implemented to solve the system. Using the Newton iterative method, the following system is obtained:

$$\mathbf{U}^{n+1} = \mathbf{U}^n - \mathbf{J}^{-1}(\mathbf{U}^n)\mathbf{R}(\mathbf{U}^n) \tag{20}$$

where

$$\mathbf{R}(\mathbf{U}) = \sum_{\alpha=1}^{8} \Psi_\alpha(\xi_I, \eta_I, \zeta_I) x_{i\alpha} - (x_i)_I \tag{21}$$

and the jacobian matrix, $\mathbf{J}(\mathbf{U}^n)$, is given by

$$J = \begin{bmatrix} \frac{\partial R_1}{\partial \xi} & \frac{\partial R_1}{\partial \eta} & \frac{\partial R_1}{\partial \zeta} \\ \frac{\partial R_2}{\partial \xi} & \frac{\partial R_2}{\partial \eta} & \frac{\partial R_2}{\partial \zeta} \\ \frac{\partial R_3}{\partial \xi} & \frac{\partial R_3}{\partial \eta} & \frac{\partial R_3}{\partial \zeta} \end{bmatrix} \tag{22}$$

The solution vector **U**, contains the natural coordinates of the point I , (ξ_I, η_I, ζ_I), at the interior of the super element.

Only the last stage is computed in the main algorithm, it is the evaluation of the second filtered values at each node inside of the independent super-elements by finite element interpolation function, calculated by the following expressions:

$$\langle \overline{v}_i \rangle_I = \sum_{\alpha=1}^{8} \psi_\alpha(\xi_I, \eta_I, \zeta_I) \overline{v}_{i\alpha} \tag{23}$$

$$\langle \overline{v}_i \overline{v}_j \rangle_I = \sum_{\alpha=1}^{8} \psi_\alpha(\xi_I, \eta_I, \zeta_I) \overline{v}_i \overline{v}_{j i\alpha} \tag{24}$$

$$\left\langle \overline{\Delta}^2 \left|\overline{S}_{ij}\right| \overline{S}_{ij} \right\rangle_I = \sum_{\alpha=1}^{8} \psi_\alpha(\xi_I, \eta_I, \zeta_I) \left(\overline{\Delta}^2 \left|\overline{S}_{ij}\right| \overline{S}_{ij} \right)_\alpha \tag{25}$$

Characteristic dimension of the test filter is calculated in the same way as of the first filter, given by Equation (12), but considering the dimensions of the independent super-elements.

As the eddy viscosity, given by Equation (13), is evaluated at the element level and the values of the dynamic coefficient, given by Equation (14), are calculated for each node of the mesh, the coefficient used for each element is the average of the nodal values of C(**x**, t). This procedure is in accordance with other authors (Oshima et al, 1996; Zang et al, 1993, Breuer and Rodi, 1994), that uses averages of C(**x**, t) to prevent abrupt variations in space and time, source of instabilities in the numerical solution. Another technique, cited by Lilly, 1992, consists of proceeding averages of the terms Mij and Lij (Equations 15) before the calculation of C(x, t), stabilizing the problem and preventing zeros in the denominator.

In this work, a limit for negative values of the eddy viscosity was adopted, which is expressed in Equation (26). The same limit was used by Zang et al, 1993.

$$\nu + \nu_t \geq 0 \tag{26}$$

Another verification adopted here is that if the denominator of the expression for C(x, t) is equal to zero, it is assumed that C(**x**, t)=0, in the corresponding node.

The dynamic model increases the total processing time between 9 and 18%, with respect to the classical Smagorinsky´s model , for the problems analyzed in this work.

3. Numerical Examples

3.2 Backward-Facing Step

Flow simulations of a two-dimensional backward-facing step with low Reynolds numbers, were initially performed in order to validate the code. The results were obtained using the Smagorinsky's model and the dynamic model. They were compared with experimental data (Armaly et al., 1983) and other numerical simulations (Silveira Neto et al., 1993; Kaiktsis et al, 1991).

The problem domain is presented in Figure 2. For the two-dimensional case, there is only one element in z direction, and the components of the velocity in this direction are equal to zero (v_3=0) over the whole flow field. The dimensions are similar to the experimental work presented by Armaly et al, 1983.

For problems characterized by Reynolds number less or equal to 1000, simulations are long enough to get the stationary average flow.

As inflow boundary conditions, a completely developed parabolic velocity profile was used (v_1=v(y), v2=0) at the entrance and none-slip condition (v1=v2=v3=0) were prescribed at the upper and lower walls. At the outflow natural boundary conditions were employed (t_1=t_2=t_3=0) (see Equation 5). Homogeneous initial conditions (v1=v2=v3=p=0)

were used, in the first simulation, for Re=100. In the other simulations the last fields of pressures and velocities calculated for previous Reynolds number were used.

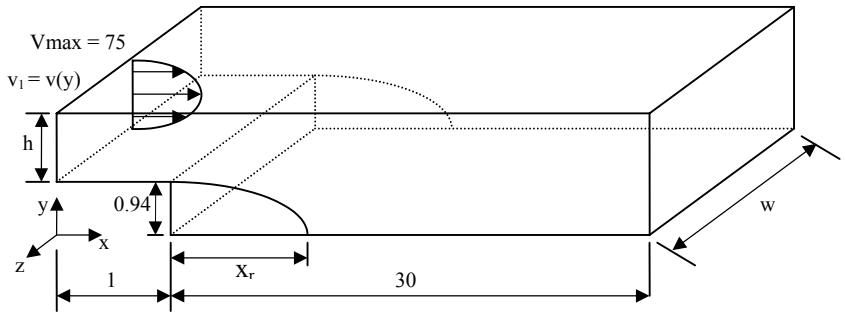

Figure 2 – Domain and characteristics dimensions of the backward-facing step.

The Reynolds number is defined in the same way that in the experiments of, being h=1.

$$Re = \frac{\rho\left(2V\,max/3\right)2h}{\mu} \tag{27}$$

To define the reattachment length it was investigated the first layer of nodes above the lower wall behind the step. The reattachment point is defined as the first node of the mesh, after the separation region (Figure 2), where the component v_1 of the average velocity field assumes a positive value. The dimensionless reattachment length is defined as Xr/H, where H is height of the step (0.94m). The results for the relation Xr/H x Re obtained at the present work, together with the values presented in Armaly, et al., 1983, are shown in Table 1.

The results for Re=100 and Re = 400 are close to those obtained experimentaly, for the two models. For laminar flows no important differences between results were expected. The dynamic model for Re=100 presented 95% of the nodes with C(**x**, t) equal to zero, the flow with Re=400 presented 94% of the nodes with C(**x**,t) equal to zero and there are not elements with negative eddy viscosity. For the flow with Re=1000, 60% of the nodes presents dynamic coefficient equal to zero, while 0.09% of the elements had negative eddy viscosity, where Equation 26 was applied.

Table 1 - Reattachment length ,Xr/H, as a function of the Reynolds number: present work x experimental work (Armaly et al, 1995).

.

X_r/H x Re			
Re	**Smagorinsky´s Model**	**Dynamic Model**	**Armaly et al. 1983 (exp.)**
100	2.74	2.89	3.0
400	7.60	7.90	8.0
1000	11.09	11.25	16.0

For Re=1000, the numerical result is far from the experimental work, this is an expected error because in two-dimensional simulations of laminar flows, characterized by Reynolds numbers grater than 500, the reattachment length is sub-estimated. The error is due to three-dimensional effects, neglected by the numerical model (Silveira Neto et, 1993, and Kaiktsis et al, 1991) and is verified by the numerical experiments of Williams and Baker, 1997.

To simulate a turbulent flow, Re=10,000 was used. At the instant of time 0,4 s, using the dynamic model, the dimensionless reattachment length was of 7.3, whereas experimental values vary between 6 and 8 (Kim et al, 1980). The number of elements where negative eddy viscosity were found was less than 6%.

Finally, results for simulations obtained with the dynamic model, for the three-dimensional flow over a backward facing step, without sidewalls, for Reynolds number 100 and 1,000, are presented. The problem domain is presented in Figure 11, where w=2. The adopted mesh is similar to that employed for the previous two-dimensional simulations, but with 8 elements in the Z direction. Boundary conditions are similar to those used in the two-dimensional case. In the first simulation it was used homogeneous initial conditions and in the following simulation the last fields of pressures and velocities calculated for the Reynolds number 100 are used as initial conditions.

As for the two-dimensional example with Re=100, the obtained reattachment length was equal to 2.88. For the flow with Re=1,000, instantaneous results can be observed in Figures 3 and 4. Despite to the low resolution in the Z direction, where only 8 elements were taken, the partial results are qualitatively coherent with the results found in other references (Silveira Neto et al., 1993; Lesieur, 1999 and Williams and Baker, 1997). The Figures 3 and 4 show that the flow is developed as expected.

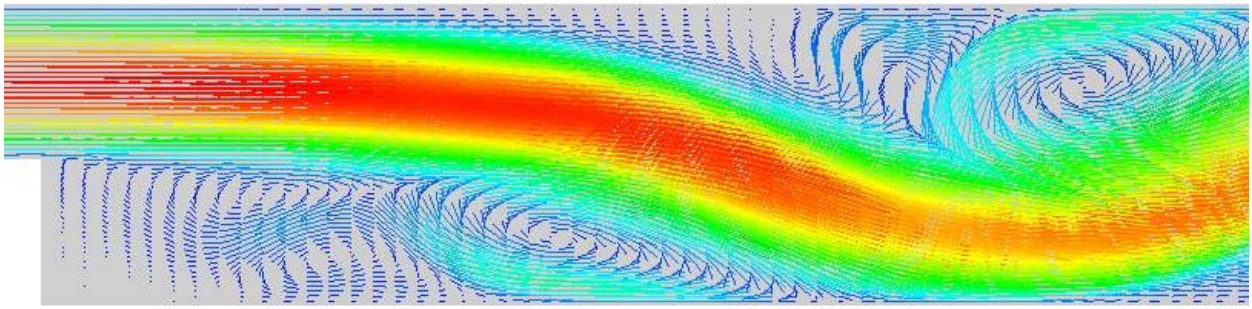

Figure 3- Detail of the velocity vectors field, in the mainstream direction at w=1.0, for the three-dimensional case with the dynamic model and Re=1,000.

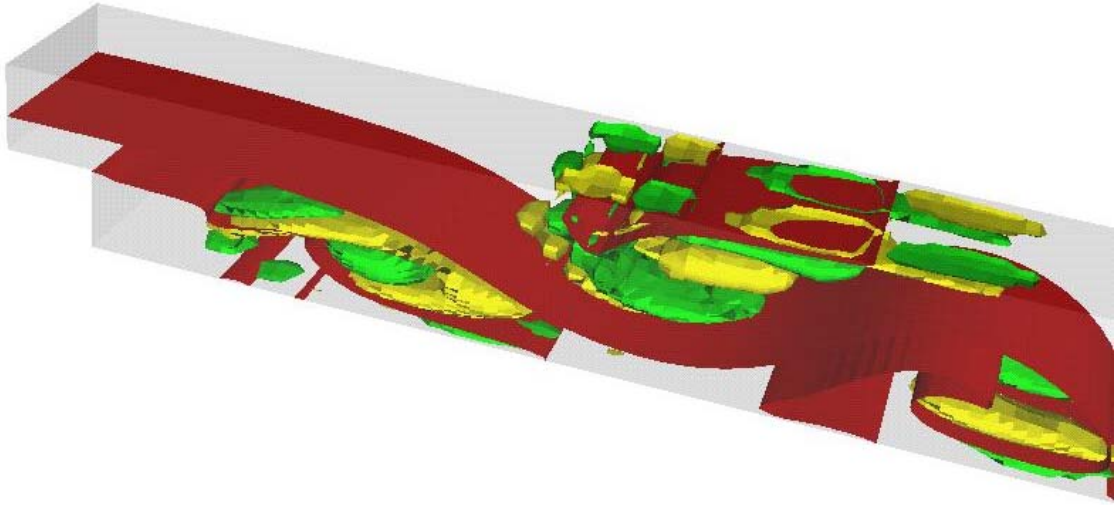

Figura 4 –Vorticity field (**w**), for Re=1,000, using the dynamic model: ♦- w_3=5.7x10^{1}, ♦-w_1=4x10^{-4} e ♦ - w_1= -4x10^{-4}.

3.2 The Driven Cavity Flow

This section presents results of three-dimensional driven cavity flow simulations for Reynolds numbers 3,200 and 10,000. This is an interesting flow, with a complex behavior in a simple geometry (figure 5), and was investigated numerically [Denaro, 1996; Kim and Menon, 1999; Zang et al., 1993] and experimentally [Prasad and Koseff, 1989] by many researchers. The experimental work of Prasad and Koseff, 1989, was used to compare present numerical study. The obtained results are close to the experimental work and have comparable quality to the numerical analysis developed by of Zang, Street and Koseff, 1993, and Kim and Menon, 1999.

The aspect ratio of the cavity flow characterized by Re=3,200 is 1 (1:1:1) while the cavity flow characterized by Re = 10,000 have aspect ratio of 0.5 (1:1:0.5). The Reynolds number is calculated based on the velocity of the upper wall U_B (Figure 5), which moves inducing the flow. All others walls are fixed, with no sleep boundary condition.

Very similar results were obtained of simulations for the complete and half domain, comparing the average velocity profiles, as well as the statistics of turbulence for Re=3200 flow with Smagorinsky´s model [Petry,2002]. Then, to reduce processing time, it is considered that the flow has a symmetry plane in H/2 (Figure 5).

3.2.1 –Three-dimensional cavity flow: Re=3200

This section presents results for three-dimensional cavity flow characterized by Re=3200 and an aspect ratio equal to 1 (B=1:D=1:H=1), assuming a symmetry plane (Figure 5). The velocity U_B is equal to 100 m/s, the sound speed, C is equal to 340 m/s and time is $\Delta t = 1.5 \times 10^{-5}$. A three-dimensional view of the mesh is presented in Figures 6. The mesh has 32x32 elements in x and y directions, refined near the walls, and has 16 elements in the z direction. The dimension of the smallest element edge is of the order of $1x10^{-2}$.

Data for the statistical analysis of turbulence was obtained storing all variables along the center lines at horizontal and vertical directions at the symmetry plane, for each time interval. The flow was analyzed until 0.795s, but for the statistical analysis it was considered the final 0.24s period.

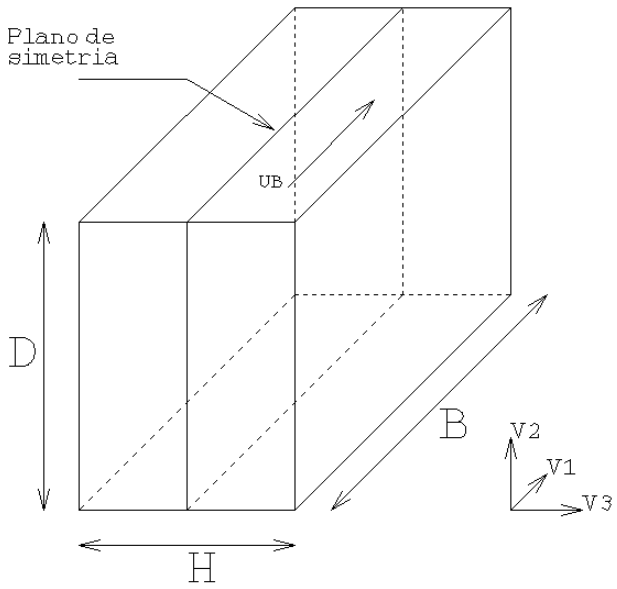

Figure 5 – Geometry of the driven cavity flow, similar of Prasad and Koseff, 1989 experimental apparatus.

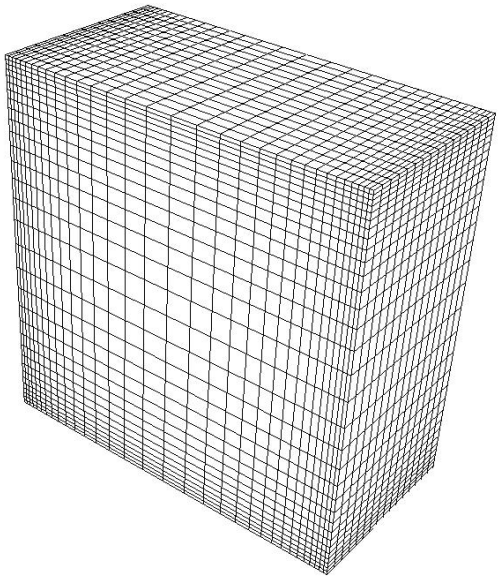

Figure 6 – Finite element mesh for the 3D cavity flow with Re=3200.

From simulations using the laminar code, and the large eddy simulation code (with Smagorinsky's and dynamic models), the profiles of average velocity components, as well as statistics of turbulence at the horizontal and vertical center lines of the symmetry plane were obtained as defined below. The experimental values presented had been token from the figures published by Prasad and Koseff, 1989.

The dimensionless mean velocity presented in Figures 7 and 11 are defined as:

$$V1 = \frac{\overline{\overline{v_1}}}{U_B} \qquad V2 = \frac{\overline{\overline{v_2}}}{U_B} \tag{28}$$

double bar indicates time average. Dimensionless forms of the root mean square, V1rms and V2rms and for Reynolds stresses UV1 and UV2 are defined in the same way as published by other autors (Zang et al., 1993 and Prasad and Koseff, 1989):

$$V1rms = 10\sqrt{\frac{\overline{\overline{v_1''^2}}}{U_B^2}} \qquad V2rms = 10\sqrt{\frac{\overline{\overline{v_2''^2}}}{U_B^2}} \tag{29}$$

$$UV1 = UV2 = 500\frac{\overline{\overline{v_1'' v_2''}}}{U_B^2} \tag{30}$$

where:

$$v_1'' = v_1 - \overline{\overline{v_1}} \qquad v_2'' = v_2 - \overline{\overline{v_2}} \tag{30}$$

Results for the mean velocity components are coincident for the three simulations (no model code and the two subgrid models codes) and have good approach with the experimental data, as it is possible to observe in Figure 7. Figures 7, 8 and 9 show results obtained in the present work, compared with the published experimental results of Prasad and Koseff, 1989.

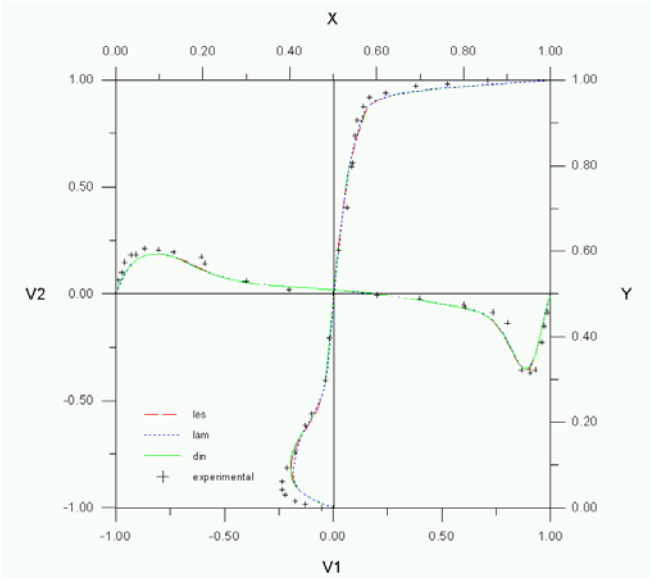

Figure 7 – Dimensionless mean velocity components profiles at center lines at the symmetry plane, Re=3200: + - experimental results [Prasad e Koseff, 1989]; - - - Smagorinsky; . . . .Laminar and ____ Dynamic models

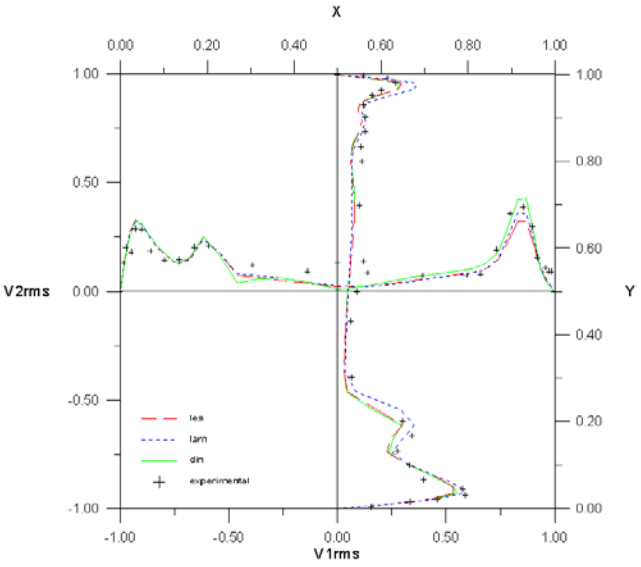

Figure 8 – Dimensionless velocity root mean square components profiles at center lines at the symmetry plane, Re=3200: + - experimental results [Prasad e Koseff, 1989]; - - - Smagorinsky; . . . .Laminar and ____ Dynamic models

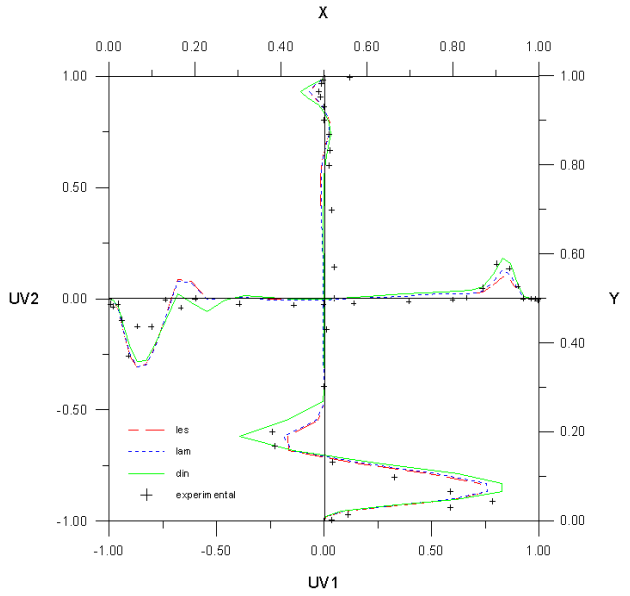

Figure 9 – Dimensionless Reynolds Stresses profiles at center lines at the symmetry plane, Re=3200: + - experimental results [Prasad e Koseff, 1989];--- Smagorinsky; . . . . . Laminar and ____ Dynamic models.

The distributions of the correlations of the velocity fluctuations, presented in figures 8 and 9, are very close to results of Prasad and Koseff, 1989. The peak of the Reynolds stresses (UV1) near the bottom wall, is more accurately captured by the dynamic model as can be verified in Figure 6. Profiles obtained clearly contain three-dimensional effects, in view of differences observed in 2d and 3d cavity flows, as presented by Prasad and Koseff, 1989.

3.1.2 Three-dimensional cavity flow: Re=10,000

Results for a three-dimensional cavity flow characterized by Re=10,000 and an aspect ratio equal to 0.5 (B=1:D=1:H=0.5), assuming a symmetry plane (Figure 5), are presented in this section. The velocity U_B is equal to 100 m/s, the sound speed, C is equal to 340 m/s and time is $\Delta t = 0.75 \times 10^{-5}$. The three-dimensional image of the mesh is presented in Figure 10. The mesh is uniform in the direction z and it is refined near walls in x and y directions. The dimension of the x and y edge of the smallest element is of the order of 5×10^{-3}.

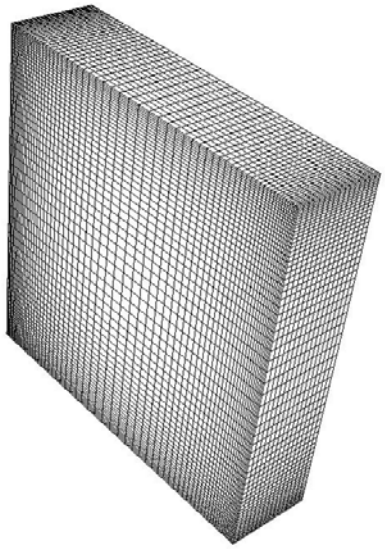

Figure 10 – Finite element mesh for 3D cavity flow with Re=10,000.

Data for the statistical analysis of turbulence was obtained storing all variables values corresponding to the center lines in the horizontal and vertical directions at the symmetry plane, for each time interval. The flow was analysed until 1.095s but for the statistical analysis it was considered the final 0. 0.6265s period. Figures 11, 12 and 13 presents dimensionless average velocity components (V1 and V2) in the center lines of the symmetry plane, as well as mean square root values (V1rms, V2rms), defined in Equations (29) and Reynolds Stresses (UV1 and UV2), defined in the Equation (30).

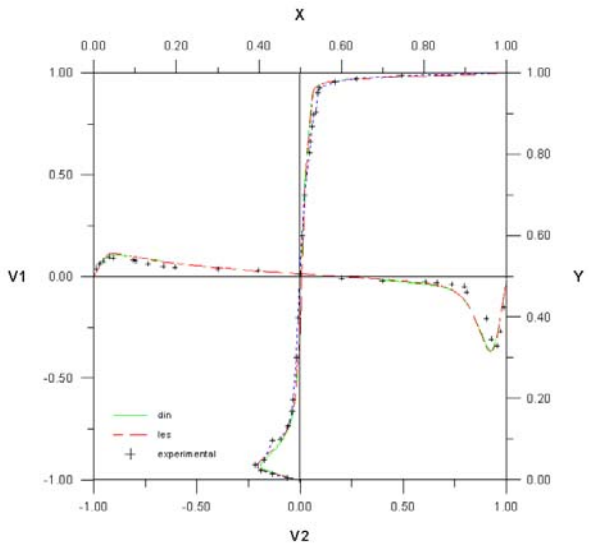

Figure 11– Dimensionless mean velocity components profiles at center lines at the symmetry plane, Re=10,000: + - experimental results [Prasad e Koseff, 1989]; - - - Smagorinsky; . . . . . Laminar and ____ Dynamic models.

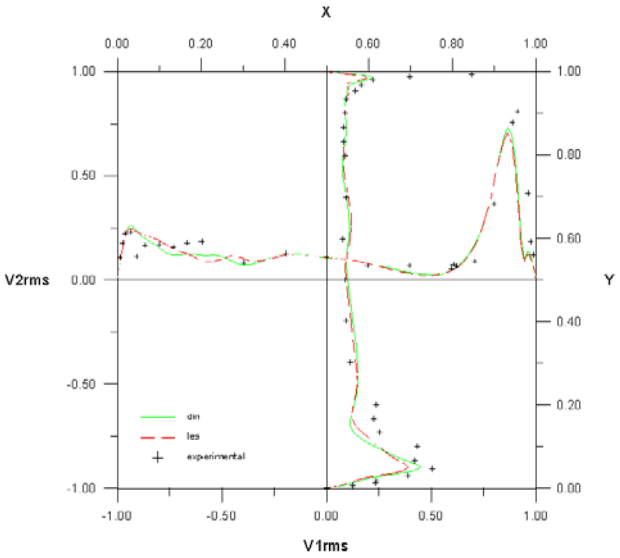

Figure 12 – Dimensionless velocity root mean square of components profiles at center lines at the symmetry plane, Re=10,000: + - experimental results [Prasad e Koseff, 1989]; - - - Smagorinsky;. . . . .Laminar and ____ Dynamic models

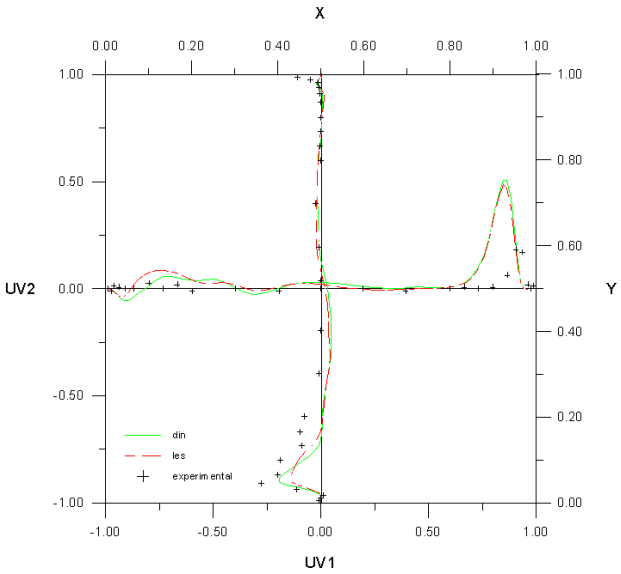

Figure 13 – Dimensionless Reynolds Stresses profiles at center lines at the symmetry plane, Re=10,000: + - experimental results [Prasad e Koseff, 1989]; - - - Smagorinsky; . . . . . Laminar and ____ Dynamic models.

Results of the present work are compared with experimental values published by Prasad and Koseff, 1989. Mean velocity results for this Reynolds number are very close to experimental results, as shown in Figure 11, for both models. In the correlations of turbulence there are differences, favorable to the dynamic model, as for example the inferior peaks, near the bottom wall of Reynolds stresses, UV1, (Figure13) and mean root square, V1rms (Figure 12). Other experiments are necessary to investigate models differences. Numerical results are comparable with other numerical results published by Zang, et al, 1993 and confirms good quality of present results.

4. Conclusions

The three dimensional classical problems of backward facing step and driven cavity flows were simulated with a Finite Element Large Eddy Simulation methodology, presented in this work. Two subgrid scale models were implemented, the Smagorinsky's and the eddy viscosity dynamic model. The results of both models are coherent with experimental and numerical data from other authors. In simulations of the backward facing step, spurious oscillations of pressure were observed and were controlled by reducing the time step, this procedure results in additional processing time witch is critical in Large Eddy Simulations. For the cavity flow problem, statistical analysis of turbulence were included and the obtained values were close to other published results, not requiring any reduction on the time step.

A new scheme for the second filtering operation in the dynamic model was presented and applied. The scheme consists of defining super-elements around each node of the original mesh and applying the finite element interpolation functions to obtain the filtered quantities for the nodes. Most of this filtering operation is developed in the pre-processing, resulting in a dynamic model with total additional cost in processing time between 9 and 18%, when compared to the implemented Smagorinsky´s model. This additional time is in the same order of the best results reported by other authors.

Analysis of the problems presented here demonstrated the capability of this methodology to simulate complex turbulent flows, without restrictions about memory allocation. The long time of processing, resulting most from the time interval restriction of this explicit scheme, indicates the relevance to improve the code before continuing the simulation of other problems in view of extended analysis of different models behavior. Researches on this aspects are in progress.

5. Acknowledgements

The authors thank the National Supercomputer Center on the Federal University of Rio Grande do Sul.

6. Bibliographic References

Armaly, B.F., Durst, F., Pereira, J.C.F., Schönung, B., 1983**.** "Experimental and Theoretical Investigation of Backward-Facing Step Flow", **Journal of Fluid Mechanics**, v. 127, pp. 473-496.

Awruch, A.M., Petry, A.P., 1997. "**On the Analysis of Viscous Incompressible Flows Using Finite Elements with the Primary Variables" (in Portuguese),** Research Report - RP 122/97, . Programa de Pós-Graduação em Engenharia Civil, Universidade Federal do Rio Grande do Sul, Porto Alegre, RS, Brazil, 73 pages.

Azevedo, R. L. 1999. "**Analysis of Fluid-Structure Interaction Problems Using the Finite Element Methot and Monolithic Coupling**"(in Portuguese). DSc Thesis . Programa de Pós-Graduacão em Engenharia Civil, Universidade Federal do Rio Grande do Sul, Porto Alegre, RS Brazil.

Burbridge, H.P., Awruch, A.M., 2000. **An efficient one-step Taylor-Galerkin Scheme to Analyze 3D High Compressible Flows Using the Finite Element Method**, Anais ENCIT 2000, Porto Alegre, RS,Brasil

Donea, J, 1984. "A Taylor-Galerkin Method for Convective Transport Problems", **International Journal for Numerical Methods in Engineering,** v 20, pp 101-119.

Ferziger, J.H.,1993. "Simulation of complex turbulent flow: recent advances and prospects in wind engineering", **Journall of Wind Engineering and Industrial Aerodynamics**, v.46 & 47, p.195-212, Elsiever.

Findikakis, A.N.; Street, R.L., 1982. "Mathematical Description of Turbulent Flows", **Journal of Hydraulics Division**, ASCE, V108, No.HY8, paper 17265, p887-903.

Germano, M. Piomelli, U., Moin, P. CabotW.H., 1991. "A dynamic sub-grid-scale eddy viscosity model", **Phys.Fluids** A3 (7), 1760-1765.

Hughes, T. J. R., 1987. **The Finite Element Method**, Prentice-Hall, New Jersey.

Kaiktsis, L., Karniadakis, G., Orzag, S.A., 1991. "Onset of three-dimensionality, equilibria, and early transition in flow over a Backward-Facing Step", **Journal of Fluid Mechanics**, v. 231, pp. 501-528.

Kawahara, M., Hirano, H.,1983. "A Finite Element Method for High Reynolds Number Viscous Fluid Flow Using Two Step Explicit Scheme". **International Journal for Numerical Methods in Fluids**, V.3, pp.137-163.

Kim, W., Menon, S., 1999. "An Unsteady Incompressible Navier-Stokes Solver for Large Eddy Simulation of Turbulent Flows". **Int. J. Numer. Meth. Fluids**, v. 31, pp. 983-1017.

Lesieur, M. Comte, P., Métais, O.,1995. "Numerical simulations of coherent vortices in turbulence", **ASME - Appl Mech Rev**, v 48, n 4.

Lilly, D.K., 1992. "A proposed moddification of the Germano subgrid-scale closure method", **Phys.Fluids A4** (3), 633-635.

Oshima, M., Kobayashi, T., Taniguchi, N., Tsubokura, M., 1996. "Development of Filtering Operation for Dynamic SGS Model Using Finite Element Method**". The Second ERCOFTAC Workshop on Direct and Large Eddy Simulation.** Septembre 16-19, 1996. Grenoble, Franca.

Padilla, E. L. M., Silveira Neto, A., 2000. "Numerical Implementation of the Dynamic Model for Turbulent Flows in Cylindrical Coordinates" (in Portuguese). **IV Simpósio Mineiro de Mecânica Computacional.** Uberlândia, MG, Brazil. pp. 573-580.

Petry, A.P., Awruch, A.M., 2003. "**Numerical Analysis of Tree-Dimensional Turbulent Flow by the Finite Element Method and Large Eddy Simulation**", In COBEM2003, 17th International Congress of Mechanical Engineering, ABCM, SP, Brazil.

Petry, A.P., 2002. "**Numerical Analysis of Tree-Dimensional Turbulent Flows Using the Finite Element Method and Large Eddy Simulation**"(in Portuguese), DSc. Thesis. Programa de Pós-Graduacão em Engenharia Mecânica, Universidade Federal do Rio Grande do Sul, Porto Alegre, RS Brazil.

Petry, A.P., Awruch, A.M., 1997. "Turbulent Flows Simulation Using the Finite Element Method and Large Eddy Simulation"(in Portuguese), **ENIEF 97,** Proceedings, San Carlos de Bariloche, Argentina.

Prasad. A. K., Koseff, J. R., 1989. "Reynolds Number and End-wall Effects on a Lid-driven Cavity Flow". **Phys. Fluids A**, v. 1, n. 2, pp 208-218.

Reddy, J.N., Gartling, D.K.. 1994. **The Finite Element Method in Heat Transfer and Fluid Dynamics**, CRC Press.

Schlichting, H. , 1968. "**Boundary Layer Theory**", McGraw-Hill, New York, 1968.

Silveira Neto, A. 2000, "Fluid Turbulence Fundamentals**", Turbulence: Proceeding of the First Spring School in Transition and Turbulence**, Editors: Freire, A.P.S. ,. Menut P.P.P e Su, J., ABCM, Rio de Janeiro, Brazil.

Silveira Neto, A., Grand, D., Métais, O., Lesieur,M., 1993. "A Numerical Investigation of Coherent Vortices in Turbulence Behind a Backward-Facing Step", **Journal of Fluid Mechanics**, v. 256, pp. 1-25.

Smagorinsky, J. 1963. "General Circulation Experiment with the Primitive Equations. I the Basic Experiment", **Monthly Weathther Review**, v. 91,n. 3, pp 99-164.

White, F.M., 1974. **"Viscous Fluid Flow"**, McGraw-Hill, New York.

Williams,P.T., Baker, A.J., 1997. "Numerical Simulations of Laminar Flow over a 3D Backward-Facing Step", **International Journal for Numerical Methods in Fluids**, v.24, pp. 1159-1183.

Zang, Y., Street, R. L., Koseff, J. R., 1993. "A Dynamic Mixed Subgrid-Scale Model and its Application to Turbulent Recirculating Flows". **Phys. Fluids A**, v. 5, n. 12, pp. 3186-3196.